Subunit Disassembly and Unfolding Kinetics of Hemoglobin Studied by Time-Resolved Electrospray Mass Spectrometry†

Douglas A. Simmons, Derek J. Wilson, Gilles A. Lajoie, Amanda Doherty-Kirby, and Lars Konermann*

Department of Chemistry, The University of Western Ontario, London, Ontario N6A 5B7, Canada

Received July 14, 2004; Revised Manuscript Received September 9, 2004

ABSTRACT: We report the use of electrospray ionization (ESI) mass spectrometry (MS) in conjunction with online rapid mixing to monitor the kinetics of acid-induced ferrihemoglobin denaturation. Under equilibrium conditions, the hemoglobin mass spectrum is dominated by the intact heterotetramer. Dimeric and monomeric species are also observed at lower intensities. In addition, ionic signals corresponding to hexameric (tetramer−dimer) and octameric (tetramer × 2) hemoglobin species are observed. These complexes may represent weak solution-phase assemblies. The acid-induced denaturation process was monitored for reaction time ranging from 9 ms to ∼3 s. The data obtained were subjected to a global analysis procedure which simultaneously fit all kinetic (ESI-MS intensity vs time) profiles to multi-exponential expressions. Results of the global analysis are consistent with the coexistence of two subpopulations of tetrameric hemoglobin which differ in their disassembly rates and ESI charge states. The higher-charge state tetramer ions preferentially dissociate via a rapid pathway ($\tau_1 = 51$ ms), resulting in the transient formation of a heme-saturated dimer, holo-α-globin, and a heme-deficient dimer. The latter is shown by MS/MS to be comprised of a heme-bound α-subunit complexed with an apo-β-chain. The slow-decaying tetramer population, apparent at a slightly lower average charge state, breaks down into its monomeric constituents with no observable intermediate species ($\tau_2 = 390$ ms). Surprisingly, unfolded apo-α-globin is formed more rapidly than unfolded apo-β-globin. The appearance of the latter occurs with a relaxation time τ_3 of 1.2 s. It is postulated that accumulation of unfolded apo-β-globin is delayed by transient population of an undetected unfolding intermediate.

Mammalian hemoglobins possess a heterotetrameric structure, comprising two pairs of heme-containing α- and β-subunits assembled in a tetrahedral arrangement. Many of the studies on this protein have been concerned with the cooperative oxygen binding behavior and concomitant structural changes, which allow hemoglobin to function as an efficient transporter of molecular oxygen (*1*, *2*). Another focus has been the exploration of rapid conformational dynamics following the photolysis of CO-bound hemoglobin (*3*, *4*). Comparatively little effort, however, has been directed toward the processes by which hemoglobin is formed from (or broken down into) its monomeric constituents (*5*). This is partially due to the structural heterogeneity of the protein, which makes association−dissociation processes very difficult for studies by optical spectroscopy. Hemoglobin exists in equilibrium among several quaternary structures, notably as monomeric (α or β), dimeric (αβ), and tetrameric ($\alpha_2\beta_2$) species (*6*, *7*). Adding to this complexity is the fact that, in principle, each of the subunits can exist in the heme-bound hologlobin form (α^h and β^h)[1] or as apoglobins (α° and β°) (*5*).

Electrospray ionization (ESI) mass spectrometry (MS) represents an attractive method for studies on large non-covalent assemblies. ESI can generate intact gas-phase ions from solution-phase complexes. Thus, ligand−protein and protein−protein assemblies can be monitored directly through the detection of the corresponding ions in the gas phase (*8*−*10*). The particular appeal of ESI-MS for the study of protein complexes is its ability to distinguish between differing quaternary structures and ligand-binding states, as well as differing solution-phase conformations (*11*, *12*). The former two are easily derived from observed masses of the complexes in the mass spectrum, whereas the latter is based on the degree of protonation acquired during ESI. While the precise nature of the charge acquisition mechanism remains unresolved, it is generally accepted that unfolded proteins acquire higher charge states than proteins in native-like, compact conformations (*13*).

Following a number of ESI-MS studies (*14*−*17*) that reported the observation of intact hemoglobin [$(\alpha^h\beta^h)_2$, denoted hereafter as Hb], Griffith and Kaltashov conducted a detailed investigation of the pH-induced denaturation of this protein under equilibrium conditions (*18*). Acidification from pH 8 to 3 resulted in a gradual decay of the Hb signal. α^h and $\alpha^h\beta^h$ were the major species observed in the mass

† This work was supported by the Natural Sciences and Engineering Research Council of Canada (NSERC), the Canada Foundation for Innovation (CFI), The Ontario Ministry of Energy, Science, and Technology, the Canada Research Chairs Program, and the University of Western Ontario.

* To whom correspondence should be addressed. Telephone: (519) 661-2111, ext. 86313. Fax: (519) 661-3022. E-mail: konerman@uwo.ca.

[1] Abbreviations: α°, apo-α-globin; β°, apo-β-globin; α^h, holo-α-globin; β^h, holo-β-globin; $\alpha^h{}^n$, multiply protonated holo-α-globin ion $[\alpha^h + nH]^{n+}$; ESI-MS, electrospray ionization mass spectrometry; Hb, tetrameric hemoglobin $(\alpha^h\beta^h)_2$; MS/MS, tandem mass spectrometry.

10.1021/bi048501a CCC: $27.50
Published on Web 10/30/2004

spectra around pH 5, along with a heme-deficient dimer (semihemoglobin, presumably $\alpha^h\beta^\circ$). Below pH 4, unfolded α° and β° chains were the dominant species. These experiments revealed distinctly different heme binding behaviors for the α- and β-subunits. The former was able to bind heme independent of quaternary association state, which is apparent by the observation of monomeric holo-α-globin. In contrast, no monomeric holo-β-globin was observed under any conditions. These data suggest that β-globin only exhibits heme binding competency while in association with α^h chains, in either a dimeric or tetrameric complex.

A thorough understanding of the mechanisms by which protein complexes assemble and disassemble requires equilibrium experiments to be complemented by kinetic studies. Assembly−disassembly processes occurring on the time scale of minutes can easily be monitored by conventional ESI-MS methods (*19*). Studies in the millisecond to second time range, however, require the use of on-line rapid mixing techniques. Our group has previously applied on-line rapid mixing ESI-MS in exploring the kinetics of protein folding and ligand binding (*20*, *21*), but never for studies on processes that involve quaternary structure changes.

In this study, this "time-resolved" ESI-MS approach is used for the first time in conjunction with a time-of-flight (TOF) mass spectrometer. The high *m*/*z* range accessible to this instrument allows the extension of rapid ESI-MS kinetic studies to large protein complexes. We use this setup for monitoring the unfolding and disassembly process of bovine ferrihemoglobin, triggered by a pH jump from neutral to acidic conditions. The overall kinetic changes follow a pattern that resembles the mechanism of acid-induced denaturation under equilibrium conditions (*18*). However, the time-dependent changes in the protein's quaternary structure, subunit conformations, and heme binding states exhibit an even higher degree of complexity.

EXPERIMENTAL PROCEDURES

Materials. Bovine ferrihemoglobin (Sigma, St. Louis, MO) was dialyzed in 10 mM ammonium acetate (Fluka, Buchs, Switzerland) prior to analysis. Consistent with previous reports, the subunit masses of the protein were found to be 15 053 and 15 954 Da for apo-α-globin and apo-β-globin, respectively (*22*). The heme group accounts for an additional 616 Da for each subunit. Acetic acid (Fisher Scientific, Nepean, ON) and HPLC-grade methanol (Caledon Laboratories, Georgetown, ON) were used without further purification. pH values were measured with an AB15 pH meter (Fisher Scientific, Nepean, ON).

ESI-MS Measurements. Kinetic experiments were performed using a capillary mixing setup that possesses an adjustable reaction chamber volume. A detailed description of this system is given in ref *23*. Briefly, this continuous-flow apparatus consists of two concentric capillaries, each of which is connected to a syringe to allow for infusion of two reactant solutions. The two solutions are mixed at the end of the inner (fused silica) capillary, and the reaction is allowed to proceed until pneumatically assisted ESI occurs at the end of the outer (stainless steel) capillary. The reaction time is controlled by the flow rates from the syringes, and by the volume between the mixing point and the end of the outer capillary. Mass spectra can be recorded for selected reaction times by acquiring data with the mixer held specific distances from the end of the outer capillary. To acquire kinetic data (i.e., intensity−time profiles), the inner capillary is withdrawn continuously such that time-dependent changes in signal intensity can be observed for all ions in the mass spectrum. For the work presented here, this setup was slightly modified to allow the coupling to an LCT time-of-flight mass spectrometer (Micromass). Hemoglobin [100 μM as a tetramer, in 10 mM ammonium acetate (pH 6.8)] and acetic acid in water (6%, v/v) were each infused at a flow rate of 30 μL/min, resulting total flow rate of 60 μL/min, and a final pH of 2.8 after mixing. Reaction times of 9 ms to 2.7 s were measured, with an additional manually mixed time point of 5 h. The mass spectrometer was operated by using elevated pressures in the ion sampling region, to facilitate the detection of large noncovalent complexes (*24*, *25*). A source pressure of 23 mbar, with sample cone and extraction cone voltages of 15 and 3 V, respectively, was found to give optimal signal intensities for the tetramer. MS/MS measurements were carried out on a Q-TOF2 quadrupole time-of-flight mass spectrometer (Micromass), which was modified to allow precursor ion selection up to *m*/*z* 8000 (*26*).

All data were collected using the MassLynx instrument software. Time-dependent changes in ion intensities were extracted from the total ion count profiles by integrating each protein peak along its entire width. Each kinetic profile was subjected to a baseline correction in which an integrated section of baseline immediately adjacent to each peak was subtracted from each intensity profile. The width of the integrated portion of the baseline was identical to that of the corresponding peak. Additionally, a correction was made to account for the distortion of the time axis due to laminar flow effects in the reaction capillary (*23*).

Global Data Analysis. Protein folding and unfolding kinetics are often described in terms of coupled first-order differential equations (*27*). This implies that a master equation of the general form (*28*)

$$\frac{d\vec{\mathbf{x}}}{dt} = \langle \mathbf{A} \rangle \vec{\mathbf{x}} \tag{1}$$

can be established, where $\vec{\mathbf{x}} = x_1(t), ..., x_n(t)$ is a vector containing all time-dependent concentrations of the *n* species that are involved in the reaction. $\langle \mathbf{A} \rangle$ is the $n \times n$ rate matrix of the system with eigenvalues $\lambda_1, ..., \lambda_n$. Except for λ_n (which is zero), the apparent rate constants λ_j are functions of all the microscopic rate constants in the matrix $\langle \mathbf{A} \rangle$. Equation 1 can be solved for any set of initial conditions, resulting in multiexponential expressions for the concentration profiles $x_j(t)$. Accordingly, any spectral signals, $I_i(t)$, accompanying the kinetics can be expressed as

$$I_i(t) = \sum_{j=1}^{n-1} C_{ij} \exp(-t/\tau_j) + C_{in} \tag{2}$$

The $n - 1$ relaxation times, τ_j, in eq 2 are given by $\tau_j = (\lambda_j)^{-1}$. These τ_j values are common to all the signal−time profiles $I_i(t)$, and the observed kinetics differ only in the amplitudes $C_{i1}, ..., C_{in}$ (*29*, *30*). Some of the τ_j values may be relatively close in magnitude. That, together with signal-to-noise limitations, and small amplitudes for some of the exponential terms, can make it difficult to resolve all the

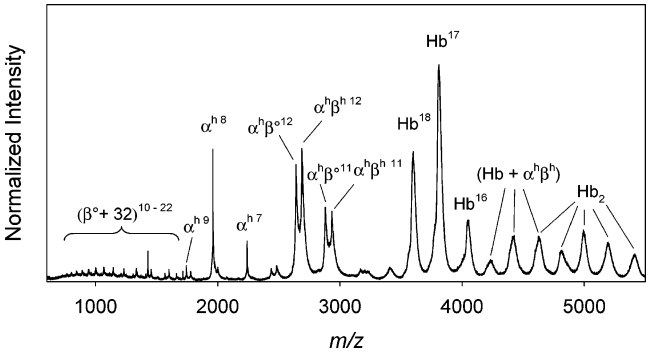

FIGURE 1: ESI mass spectrum of 100 μM (as tetramer) hemoglobin in 10 mM ammonium acetate (pH 6.8). Intact tetramer ions are denoted Hb. Association of a heme group with either α- or β-globin is denoted with a superscript h.

$n - 1$ relaxation processes. In this work, it was found that the intensity profiles for all ESI-MS signals observed during hemoglobin denaturation could be described by the sum of three exponentials, in addition to a constant term.

$$I(m/z,t) = a_1(m/z)\exp(-t/\tau_1) + a_2(m/z)\exp(-t/\tau_2) + a_3(m/z)\exp(-t/\tau_3) + a_4(m/z) \quad (3)$$

$I(m/z,t)$ is the integrated ESI-MS intensity for each peak at time t, and τ_1, τ_2, and τ_3 are relaxation times with amplitudes $a_1(m/z)$, $a_2(m/z)$, and $a_3(m/z)$, respectively, and $a_4(m/z)$ is a nondecaying component. Following the global analysis concept, the three relaxation times were required to be the same for all the $I(m/z,t)$ data, and they were determined by fitting the entire set of kinetic profiles simultaneously (*31*). Only parameters $a_1(m/z)$, $a_2(m/z)$, $a_3(m/z)$, and $a_4(m/z)$ were allowed to vary for each profile. In addition to drastically reducing the number of parameters to be determined, the global analysis procedure significantly increases the accuracy of the relaxation times by using data from all of the observed protein states, rather than from a single peak (*29*, *32*). Overall, the relative error of each fitted relaxation time was found to be around 10%. The fitting procedure employed a least-squares routine that is based on the usage of a genetic algorithm (*33*).

RESULTS AND DISCUSSION

ESI-MS of Native Hemoglobin. Figure 1 shows the ESI mass spectrum of 100 μM hemoglobin recorded at equilibrium in 10 mM ammonium acetate at pH 6.8. This spectrum is consistent with data obtained in earlier ESI-MS studies (*14*−*18*, *22*). A careful investigation of the ionic signals observed under these native solvent conditions is necessary for a proper interpretation of the subsequent time-resolved data. The spectrum exhibits a considerable degree of heterogeneity. As expected, it is dominated by the Hb tetramer in protonation states +16 to +18. Also prominent in Figure 1 are peaks corresponding to $\alpha^h\beta^h$ in charge states +11 and +12, along with a similarly charged heme-deficient dimer (labeled $\alpha^h\beta^\circ$). As previously discussed by Griffith and Kaltashov (*18*), it is unlikely that these dimers and monomers are artifacts of the ESI process. Consequently, these ions are believed to be a reflection of dimeric and monomeric protein species in solution.

The mass spectrum in Figure 1 shows several peaks above m/z 4100. Although the occurrence of these signals has been reported previously (*18*), their subunit composition has not been elucidated. The assignment of these ions is difficult due to poor desolvation, a complication that is commonly encountered for ESI-MS studies on large protein complexes (*34*). To promote declustering, and thereby enhance peak shape, hemoglobin solutions containing 25% (v/v) methanol, a solvent known to be highly amenable to ESI (*35*), were prepared. Panels B and C of Figure 2 show the high-m/z portion of the hemoglobin spectrum in 25% methanol, at cone voltages of 25 and 95 V, respectively. The presence of methanol did not significantly alter the observed charge state distributions compared to that of the aqueous sample (Figure 2A). However, in conjunction with an increase in the cone voltage, the presence of methanol resulted in significantly improved desolvation. On the basis of Figure 2C, the group of peaks centered around m/z 4400 can be assigned to hexamers, having a Hb + $\alpha^h\beta^h$ composition. Ions around m/z 4900 represent octameric complexes (Hb_2). Both hexamer and octamer ions appear in a series of consecutive charge states. An interesting question is how these two gas-phase assemblies are related to protein quaternary structures in solution. The observation of protein complexes in ESI-MS that are larger than those expected on the basis of solution-phase data is not unprecedented. For example, gel filtration experiments on vanillyl-alcohol oxidase showed that protein to exist predominantly as an octamer. ESI-MS studies revealed the presence of the expected octamers, but in addition, 16-mers and 24-mers were observed (*36*). While the exact nature underlying this phenomenon must await future clarification, it seems possible that these unexpectedly large complexes observed in ESI-MS do represent loosely

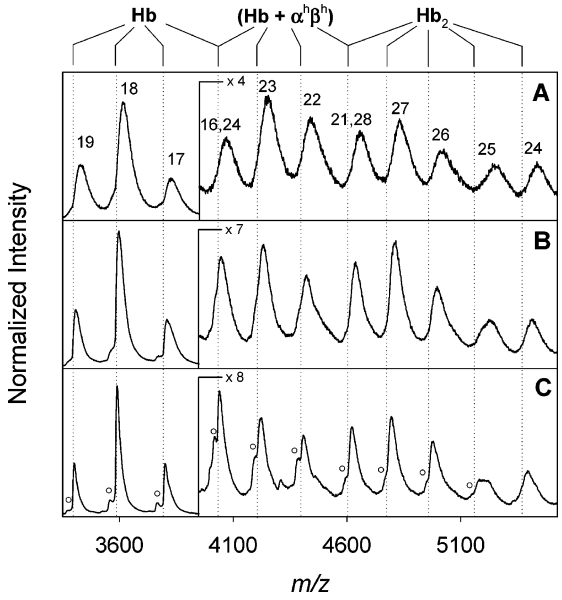

FIGURE 2: High-m/z region of the mass spectra of hemoglobin in 0% (A) and 25% (B and C) methanol, at cone voltages of 25 V (A and B) and 95 V (C). Intensities for m/z >3950 have been magnified to allow clearer illustration. Dotted lines show the calculated positions for peaks corresponding to Hb, Hb + $\alpha^h\beta^h$, and Hb_2 in various charge states as indicated. For peaks which possibly result from two different complexes, charge states corresponding to both species are given. Circles in panel C mark peak shoulders corresponding to the loss of a single heme by collision-induced dissociation in the gas phase. The charge state distributions of Hb, Hb + $\alpha^h\beta^h$, and Hb_2 are slightly shifted in this figure compared to Figure 1 due to the use of a different type of mass spectrometer (Q-TOF2 here vs LCT in Figure 1).

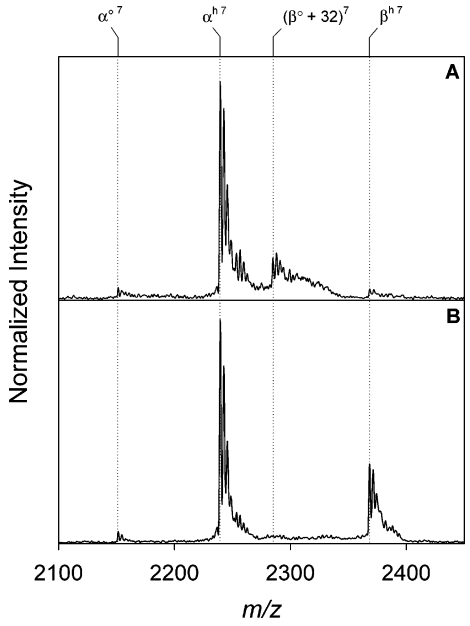

FIGURE 3: Representative portion of tandem mass spectra (fragment ion scans) for $\alpha^h\beta^{o\,12}$ (A) and $\alpha^h\beta^{h\,12}$ (B) at a collision voltage of 25 V.

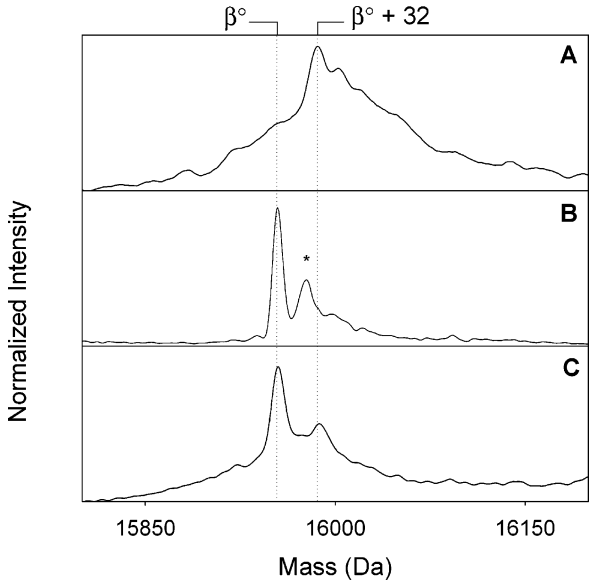

FIGURE 4: Mass distributions for β° obtained under different conditions. (A) β° observed under the "native" solvent conditions described in the legend of Figure 1, representing unfolded solution-phase apo-β-globin. (B) β° as the MS/MS product (fragment ion) of Hb^{18}, using a collision voltage of 70 V (the asterisk denotes a sodium adduct). (C) β° observed for acid-denatured hemoglobin (see Figure 5D). The expected masses of unmodified apo-β-globin (β°) and modified protein ($\beta^\circ + 32$) are given.

associated solution-phase assemblies that go undetected in conventional chromatographic and/or spectroscopic studies.

Another interesting feature in the hemoglobin equilibrium spectrum is the heme-deficient dimer in charge states +11 and +12, which has tentatively been assigned to the $\alpha^h\beta^\circ$ subunit structure in Figure 1. In principle, it could also have the $\alpha^\circ\beta^h$ composition, or it could be a mixture of $\alpha^h\beta^\circ$ and $\alpha^\circ\beta^h$. These three scenarios would be indistinguishable in standard ESI-MS experiments. MS/MS was therefore employed to confirm the subunit composition of the heme-deficient dimer. Selective fragmentation of the heme-deficient dimer in the gas phase predominantly produced α^h and β° ions in various charge states (the latter was observed to be shifted by +32 Da; this phenomenon is addressed below). A representative portion of the MS/MS spectrum is depicted in Figure 3A. As a control, MS/MS fragmentation of the holodimer ($\alpha^h\beta^h$) was also performed, resulting in α^h and β^h being the dominant collision products (Figure 3B). This second fragmentation experiment serves to prove that the stability of heme−protein interactions in both α^h and β^h is sufficient for their survival during the dissociation of the protein dimer in the gas phase. From these data, it is concluded that the heme-deficient dimer ions in Figure 1 do indeed have the $\alpha^h\beta^\circ$ subunit composition.

Given the known tendency of hemoglobin to assemble into a tetrameric quaternary structure, the observation of relatively strong signals corresponding to monomeric β° and α^h proteins in Figure 1 is somewhat surprising. α^h ions appear in relatively low charge states (+7 to +9), thus representing a tightly folded heme-bound solution-phase conformation. β° ions in significantly higher charge states represent unfolded heme-free apo-β-globin (*18*, *20*, *37*). Close inspection of these highly charged β° ions reveals that they predominantly correspond to a mass that is 32 Da higher than the expected mass ($\beta^\circ + 32$, MW = 15 986 Da; Figure 4A). β° ions with the expected mass only appear as a relatively weak shoulder on the low-*m*/*z* side of the main peak. It is very likely that the observed mass increase is due to the oxidation of two methionine side chains, resulting in a shift of +16 Da per oxidation (*38*, *39*). The β-subunit contains three methionyl residues, all of which appear to be solvent-exposed in the X-ray structure of hemoglobin. In contrast, α-globin, for which no modification is observed, possesses only a single methionine residue that is buried deep within the tertiary structure (*40*). We are currently trying to confirm this oxidation hypothesis through MS/MS studies on hemoglobin peptide maps.

It is interesting to explore the involvement of this (β + 32) species in the various hemoglobin quaternary complexes. The poor desolvation of the peaks above *m*/*z* 2400 precludes unambiguous mass assignments in this range, and therefore, MS/MS had to be employed. β° released upon gas-phase fragmentation of the Hb tetramer exclusively appears in the unmodified form (Figure 4B). The same result was obtained upon fragmentation of $\alpha^h\beta^h$, Hb_2, and Hb + $\alpha^h\beta^h$ (data not shown). Only the fragmentation of $\alpha^h\beta^\circ$ predominantly results in the release of modified β-subunits (Figure 3A). The relative contribution of the modified protein in this case is on the order of 60−80% (an accurate quantification is difficult due to the appearance of sodium adducts). These results show that, while able to associate with α^h to form a heme-deficient dimer, modified β° chains are incapable of binding heme and, consequently, not competent for holodimer or tetramer formation. The binding affinity of modified β-globin for α^h appears to be relatively low, as seen by the considerable amount of monomeric $\beta^\circ + 32$ ions in Figure 1. To assess the overall ratio of unmodified versus modified β-subunits in the hemoglobin sample, the protein solution was acidified to pH 2.8, resulting in unfolding, subunit disassembly, and heme loss for all subunits (see below; Figure 5D). The mass distribution of β° under these conditions reveals the presence of ca. 15% modified protein (Figure 4C).

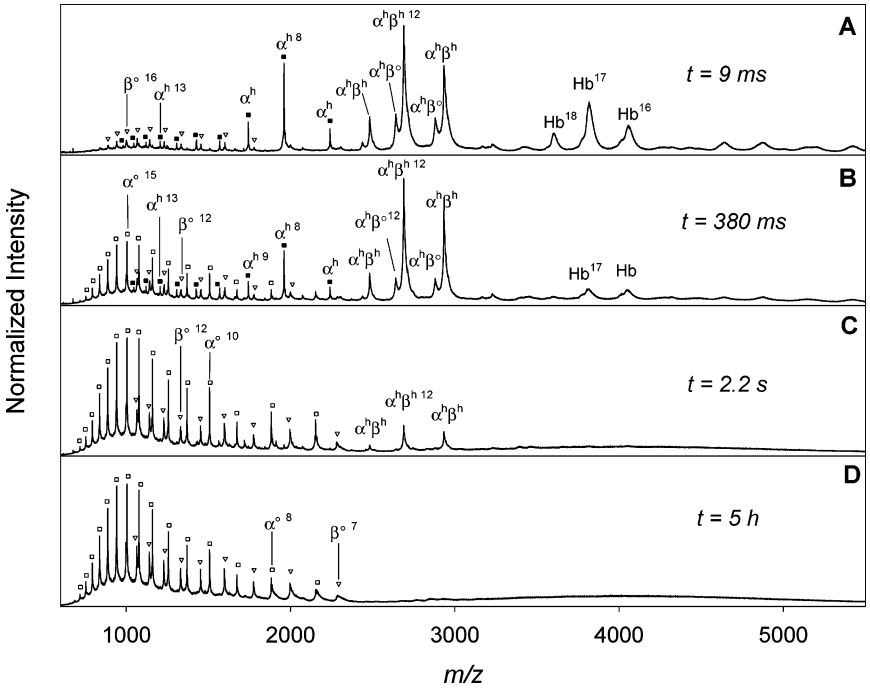

FIGURE 5: Time-resolved mass spectra recorded at selected times following the initiation of acid-induced hemoglobin denaturation. Selected charge states are given for reference: (□) α°, (■) α^h, and (▽) β°.

Time-Resolved ESI-MS. Mass spectra recorded at selected times during acid-induced denaturation of hemoglobin are shown in Figure 5. The first of these spectra, obtained after the sample had been exposed to acid for 9 ms (Figure 5A), already shows significant changes compared to the equilibrium spectrum prior to acid exposure. Most notably, the relative contribution of $\alpha^h\beta^h$ is drastically increased. In addition, small signals for high-charge (+11 to +17) α^h are visible, indicating that some of the monomeric holo-α-globin is present in a more extended conformation while still maintaining contact with the heme group. No unligated α-chains are visible at this time point, which shows that unfolding of holo-α-globin occurs prior to heme dissociation. This behavior of α-globin is consistent with what has been observed during acid-induced unfolding of the structurally similar myoglobin (*41*).

After denaturation for 380 ms (Figure 5B), the contributions of Hb tetramer and larger oligomers are significantly diminished, while $\alpha^h\beta^h$ remains the dominant species. α° in a wide range of different charge states below *m*/*z* 1800 represents a structurally heterogeneous apo-α-globin population. After 2.2 s (Figure 5C), the dominant peaks in the spectrum correspond to α° and β°. The multimodal charge state distributions observed for α- and β−chains indicate the coexistence of two or more conformations for each subunit (*42*, *43*). A spectrum recorded after hemoglobin had been kept at pH 2.8 for 5 h is depicted in Figure 5D. It shows α° and β° ions in high-charge states, centered around +15. This spectrum represents the end point of the acid-induced denaturation process, where all the quaternary assemblies have broken down, the native heme−protein interactions are disrupted, and all the proteins adopt a largely unfolded conformation. It is noteworthy that the relative contribution of modified versus unmodified β° is heavily weighted toward the latter by this time (see Figure 4C). β° signal intensities discussed in the subsequent sections refer to the unmodified form of the protein.

Kinetic Profiles. Operated in continuous-withdrawal mode (*23*), the rapid mixing apparatus employed in this study generates kinetic (intensity vs time) profiles for all the observed ionic species (*23*). This provides a valuable complement to the time-resolved mass spectra of Figure 5, and allows some insight into the mechanistic details of hemoglobin denaturation.

It is undisputed that individual bell-shaped protein charge state envelopes in ESI-MS can be assigned to ensembles of polypeptide chains that share a similar overall solution-phase structure (*13*). However, it is not entirely clear whether, within a given charge envelope, higher charge states reflect a higher degree of unfolding. For monomeric proteins, there is evidence to suggest that adjacent peaks can represent slightly different conformations (*20*). However, for multiprotein complexes, there do not seem to be any previous data to support this notion. Figure 6 shows a comparison of the kinetic profiles recorded for the three major charge states of the hemoglobin tetramer. The observed curves are different for each charge state, with the rate of decay increasing with an increase in charge. This result strongly suggests that the charge state envelope of the Hb tetramer arises from more than one conformational state, rather than from a uniform ensemble of solution-phase tetramers. Complexes giving rise to the +18 charge state appear to represent structures which are not as resilient to acidic pH as those being represented by the +16 charge state. This interpretation is consistent with the idea that even the native state of a protein (or of a protein complex) is an ensemble of different conformations (*44*). The intermediate kinetics of the +17 charge state may result from overlapping contributions from fast- and slow-decaying Hb subpopulations which, in the following discussion, will be termed Hb_{fast} and Hb_{slow}, respectively.

Kinetic profiles for selected charge states of other major species observed during hemoglobin denaturation are shown in Figure 7. Decay kinetics for the octamer (Figure 7A) and hexamer (Figure 7B) are qualitatively similar to those of the

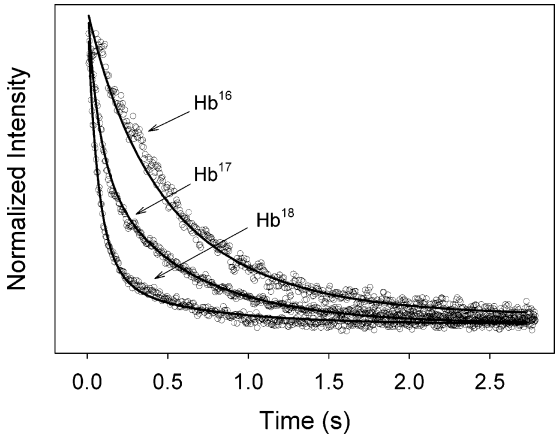

FIGURE 6: Decay kinetics of the hemoglobin tetramer, monitored in the +16, +17, and +18 charge states. Experimental data correspond to the baseline-corrected intensity profiles observed for each charge state. Solid lines represent fits to the experimental data which were generated by a global analysis fitting procedure.

tetramer; however, no clear correlation was observed between charge state and decay rate. The profiles for $\alpha^h\beta^h$ (Figure 7C) are characteristic of a reaction intermediate; a formation phase is observed if $t < 100$ ms, followed by a slower decay in intensity. Behavior consistent with a reaction intermediate was also observed for low- and high-charge α^h, as well as for $\alpha^h\beta^\circ$ (panels E, F, and D of Figure 7, respectively). MS/MS studies revealed that the relative contribution of unmodified β° in the heme-deficient dimer increased with an increase in reaction time (data not shown). Panels G and H of Figure 7 represent the formation of the final products of the denaturation process, i.e., unfolded apo-α-globin and apo-β-globin. The α° profile shows a lag phase which extends for roughly the first 100 ms after mixing. It is during this period that the intermediate species (panels C−F of Figure 7) achieve their maximum population. On the same time scale, all the β° profiles show a characteristic "hook", i.e., a rapid decrease in intensity, that is followed by a much slower rise. The origin of this interesting behavior (exemplified for $\beta^{\circ 13}$ in Figure 7H) will be discussed below. None of the other species showed this feature.

Global Data Analysis. Processing of the kinetic data for all species was performed using the analysis procedure outlined in Experimental Procedures. It was found that a minimum of three exponentials, in addition to a constant term, provided satisfactory fits to the entire set of kinetic profiles. The solid lines in Figures 6 and 7 provide examples of the fits that were obtained using this strategy. The relaxation times in eq 3 were calculated: $\tau_1 = 51$ ms, $\tau_2 = 390$ ms, and $\tau_3 = 1.2$ s. The amplitude spectra depicted in Figure 8 represent the contributions of each relaxation time to the kinetics observed for every ionic species. Negative amplitudes correspond to an intensity increase (i.e., the formation of a species). Conversely, positive amplitudes represent a decay in intensity, or a lag in formation.

Figure 8A shows the $\tau_1 = 51$ ms amplitude spectrum. Decay components corresponding to this relaxation time were observed for Hb_2 and Hb + $\alpha^h\beta^h$, as seen from the positive amplitudes for this species. Similarly, this relaxation time was found to contribute to the rapidly decaying tetramer (Hb_{fast}) in the +17 and +18 charge states. No significant amplitude was found for the +16 charge state of the tetramer (Hb_{slow}). Large negative amplitudes were observed for $\alpha^h\beta^h$, which indicates that this holodimer is a major product of the decay processes affecting Hb_2, Hb + $\alpha^h\beta^h$, and Hb_{fast}. Negative amplitudes for α^h in various charge states represent the formation of holo-α-globin in various conformations.

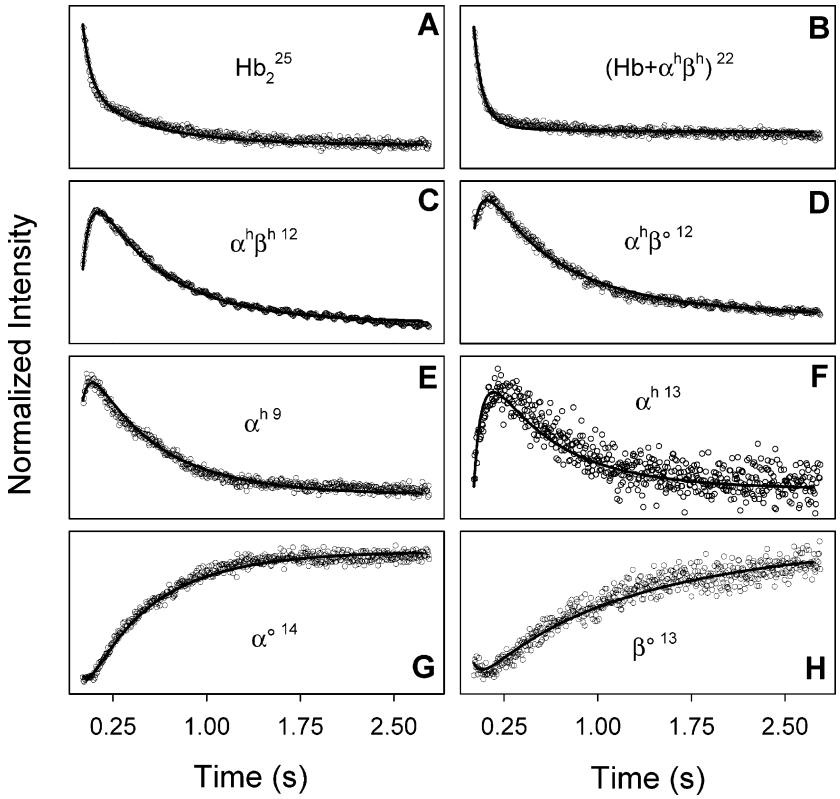

FIGURE 7: Kinetic profiles for selected species observed during acid-induced hemoglobin denaturation. For additional information, see the legend of Figure 6.

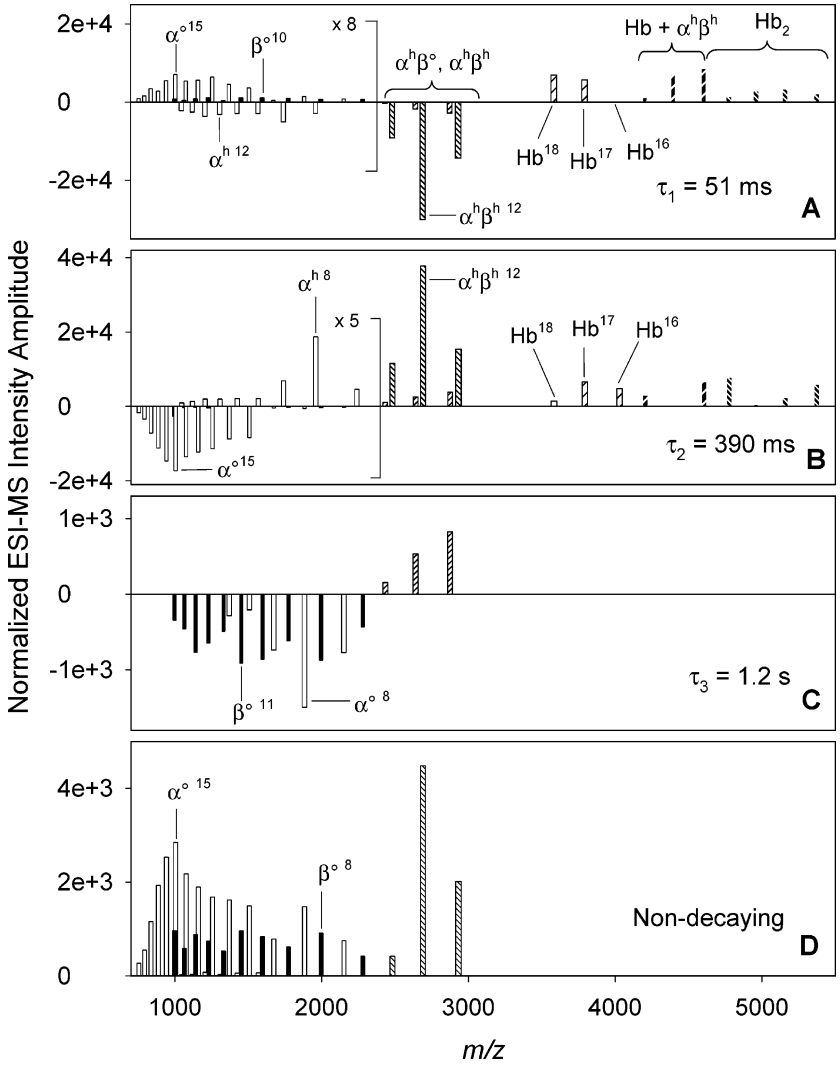

FIGURE 8: Amplitude spectra for the exponential relaxation times observed during acid-induced denaturation of hemoglobin, as obtained from global analysis. Positive amplitudes correspond to the occurrence of a decay or a lag phase; negative amplitudes represent the formation of a species.

Positive amplitudes for α° ions in high-charge states represent the lag phase in the formation of unfolded apo-α-globin (see Figure 7G). The small positive amplitudes for *β*° in Figure 8A represent the hook feature exhibited by the kinetic profiles of apo-*β*-globin (see Figure 7H).

The amplitudes for the second relaxation component (τ_2 = 390 ms) are shown in Figure 8B. Significant positive amplitudes are observed for Hb_2 and Hb + $\alpha^h\beta^h$. Also, Hb tetramers undergo a decay process corresponding to this relaxation time, including ions in the +16 charge state (Hb_{slow}). In addition to Hb_{slow}, a host of other α^h-containing species ($\alpha^h\beta^h$, $\alpha^h\beta$°, and α^h in both low- and high-charge states) undergo a decay process on the time scale of τ_2, with concomitant formation of unfolded apo-α-globin, as seen from the negative amplitudes for α°. The fact that all these kinetic processes share the same relaxation time may point to a common rate-determining step, possibly the opening of the α-globin heme-binding pocket, with concomitant heme release.

A third relaxation time (τ_3 = 1.2 s) with relatively small amplitudes is required to adequately describe a slow phase of the $\alpha^h\beta$° decay, and the concurrent formation of a subpopulation of monomeric globin species. The formation of α° on this time scale is limited to the lower-charge states, corresponding to the formation of a more folded conformation of apo-α-globin. In addition, apo-*β*-globin in various unfolded conformations appears with relaxation time τ_3.

Finally, the amplitudes of the "nondecaying" component are shown in Figure 8D. This spectrum represents an extrapolation of the relative ion abundances for infinite time, based on the exponential expressions determined during global analysis for the ~3 s experimental time window. Comparison of Figure 8D with the actual t = 5 h spectrum (Figure 5D) reveals a major difference only with respect to $\alpha^h\beta^h$. It is apparent that this holodimer undergoes an additional very slow decay process that is beyond the time range accessible to our rapid mixing technique.

The amplitude spectra depicted in Figure 8 reveal a puzzling phenomenon, namely, a pronounced imbalance between the total quantity of α and *β* species that are formed by the various processes associated with the three relaxation times. The overall stoichiometric α:*β* ratio in hemoglobin is unity. The formation of α^h in Figure 8A, for example, should therefore be accompanied by the formation of a *β* species. However, no such process is observed. Similarly, the decay of Hb_2, Hb + $\alpha^h\beta^h$, Hb_{slow}, and $\alpha^h\beta^h$ in Figure 8B generates monomeric α°, as seen by the negative amplitudes for that species, whereas near-zero amplitudes are observed for the

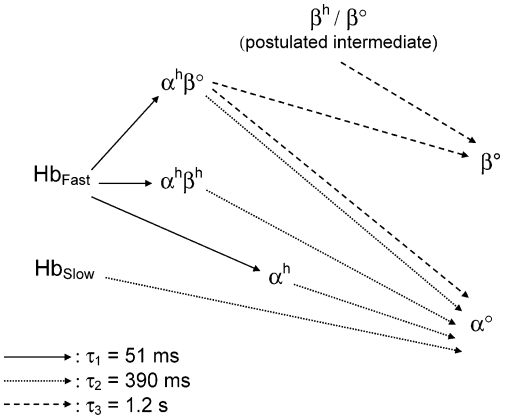

FIGURE 9: Summary of the hemoglobin disassembly and unfolding process, as determined by global analysis. Arrows represent processes associated with the three relaxation times. Also given is the postulated (undetected) β-containing transient intermediate.

accompanying formation of $\beta°$. Virtually all of the $\beta°$ intensity is generated on the slow time scale of τ_3 (Figure 8C). The only decay with this relaxation time is that of $\alpha^h\beta°$; however, it is clear that this process cannot be the sole source of all the monomeric apo-β-globin. The overall α/β imbalance is also apparent from the intensity profiles in panels G and H of Figure 7, which show that unfolded apo-β-globin is generated considerably more slowly than unfolded apo-α-globin. Another interesting observation is that, consistent with several previous studies (*17*, *18*, *45*, *46*), Figure 5D shows much lower signal intensities for acid-denatured apo-β-globin than for apo-α-globin. It is noted that the presence of ~15% modified (β + 32)-globin in the sample is by far not sufficient to account for this effect.

To rationalize the α:β imbalance in the observed kinetics, we postulate the involvement of a β (or β-containing) reaction intermediate that goes undetected during ESI-MS. This species may still be populated to some extent under acidic equilibrium conditions, thus accounting for the low $\beta°$ ion intensities in Figure 5D. The kinetic data provide considerable support for the occurrence of such an intermediate. Prior to acid exposure of the protein, some apo-β-globin in high charge states is observable in the mass spectrum (Figure 1). The conspicuous "hooks" in the $\beta°$ profiles represent a decay of these initial ion intensities during the first 150 ms of the reaction (Figure 7H). This decay is consistent with the formation of a solution-phase form of β-globin that has a very low ionization efficiency. The formation of such a species does not seem impossible, taking into consideration how changes in protein conformation, along with the nature of solvent-exposed side chains, can dramatically affect signal intensities during ESI-MS (*47*, *48*). In addition, the known tendency of monomeric β-globin to undergo aggregation may play a role (*49*, *50*). To account for the kinetic α:β imbalance, we postulate that much of the nascent monomeric β-globin, generated during the breakdown of the various quaternary structures, does initially form this low-ionization efficiency species with a rate constant close to τ_1^{-1}. The slow reappearance of high-charge state $\beta°$ signal intensity (starting after ~200 ms, Figure 7H) is assigned to the conversion of this putative intermediate to a more readily ionizable unfolded solution-phase conformation.

Proposed Mechanism of Hemoglobin Denaturation. Figure 9 summarizes the relationships between the various observed species, as determined from the kinetic amplitude spectra. Most importantly, two subpopulations of hemoglobin tetramers, Hb_{fast} and Hb_{slow}, have to be distinguished. These two species undergo denaturation in parallel, but follow different pathways. Hb_{fast} represents a less tightly folded structure that forms higher-charge states in ESI-MS. It preferentially undergoes disassembly with a relaxation time τ_1 of 51 ms (solid arrows in Figure 9), resulting in the formation of $\alpha^h\beta^h$ as a major intermediate. In addition, α^h is formed, which appears in two different charge state distributions that reflect different degrees of unfolding. A relatively small amount of $\alpha^h\beta°$ is also generated from the decay of Hb_{fast}.

The dotted arrows in Figure 9 represent processes associated with a τ_2 of 390 ms. These include the formation of unfolded apo-α-globin from Hb_{slow}, $\alpha^h\beta^h$, $\alpha^h\beta°$, and α^h. The third relaxation time (τ_3 = 1.2 s) leads to the population of unfolded apo-β-globin from a postulated intermediate. In addition, unfolded apo-β-globin is formed through the disassembly of $\alpha^h\beta°$, which also releases apo-α-globin in a relatively compact conformation. No attempt was made to incorporate the formation of the putative β-globin intermediate in the reaction scheme of Figure 9. Also, hexamers and octamers were not included. These larger species may correspond to loosely associated solution-phase assemblies, corresponding to combinations of Hb_{fast}, Hb_{slow}, and $\alpha^h\beta^h$. Such a scenario would explain why the decay processes of hexamers and octamers occur with the same relaxation times as decays of $\alpha^h\beta^h$ and Hb.

CONCLUSIONS

Hemoglobin is a highly heterogeneous system, existing as a complex mixture of several quaternary structures, conformations, and heme-binding states. Most traditional spectroscopic techniques generate structural information averaged across the entire protein population. Consequently, detailed studies of the dynamics of heterogeneous multiprotein complexes by these conventional approaches are challenging. Here, time-resolved ESI-MS was used to examine the denaturation kinetics of hemoglobin. Analysis of the decay and formation of various hemoglobin species following a pH jump allowed the development of a detailed mechanism of the overall processes. By and large, the disassembly kinetics resemble the progression of hemoglobin denaturation observed under equilibrium conditions (*18*). The fundamental structural entities formed by hemoglobin are heterotetramers, heterodimers, and monomers. Trimeric species and homodimers are not observed. Despite their high degree of sequence homology, the α- and β-subunits show a very different kinetic behavior. However, the exact role of β-globin cannot be delineated with certainty at this point, as the kinetic data strongly suggest the formation of an undetected intermediate. Other intermediates are clearly observable; these include $\alpha^h\beta^h$ and $\alpha^h\beta°$, in addition to holo-α-globin in at least two different solution-phase conformations. The observation of intermediates during the unfolding kinetics of monomeric proteins is well-established (*51*). In contrast, there appear to be few previous data on the occurrence of transient species during the unfolding of quaternary protein structures. Overall, this work demonstrates the utility of time-resolved ESI-MS for kinetic studies on multiprotein complexes. Investigations into the currently

unresolved kinetic mechanism of hemoglobin reconstitution, as well as dissociation−association processes of other protein complexes, should be well-suited to the approaches used in this study.

ACKNOWLEDGMENT

We thank Doug Hairsine for providing expert support with operation of the LCT mass spectrometer.

REFERENCES

1. Eaton, W. A., Henry, E. R., Hofrichter, J., and Mozzarelli, A. (1999) Is cooperative oxygen binding by hemoglobin really understood, *Nat. Struct. Biol. 6*, 351−358.
2. Englander, J. J., Del Mar, C., Li, W., Englander, S. W., Kim, J. S., Stranz, D. D., Hamuro, Y., and Woods, V. L., Jr. (2003) Protein structure change studied by hydrogen−deuterium exchange, functional labeling, and mass spectrometry, *Proc. Natl. Acad. Sci. U.S.A. 100*, 7057−7062.
3. Jayaraman, V., Rodgers, K. R., Mukerji, I., and Spiro, T. G. (1995) Hemoglobin Allostery: Resonance Raman Spectroscopy of Kinetic Intermediates, *Science 269*, 1843−1848.
4. Adachi, S.-I., Park, S.-Y., Tame, J. R. H., Shiro, Y., and Shibayama, N. (2003) Direct observation of photolysis-induced tertiary structural changes in hemoglobin, *Proc. Natl. Acad. Sci. U.S.A. 100*, 7039−7044.
5. Vasudevan, G., and McDonald, M. J. (2002) Ordered heme binding ensures the assembly of fully functional hemoglobin: a hypothesis, *Curr. Protein Pept. Sci. 3*, 461−466.
6. Edelstein, S. J., Rehmar, M. J., Olson, J. S., and Gibson, Q. H. (1970) Functional aspects of the subunit association-dissociation equilibria of hemoglobin, *J. Biol. Chem. 245*, 4372−4381.
7. Griffon, N., Baudin, V., Dieryck, W., Dumoulin, A., Pagnier, J., Poyart, C., and Marden, M. C. (1998) Tetramer-dimer equilibrium of oxyhemoglobin mutants determined from auto-oxidation rates, *Protein Sci. 7*, 673−680.
8. Rostom, A. A., Fucini, P., Benjamin, D. R., Juenemann, R., Nierhaus, K. H., Hartl, F. U., Dobson, C. M., and Robinson, C. V. (2000) Detection and selective dissociation of intact ribosomes in a mass spectrometer, *Proc. Natl. Acad. Sci. U.S.A. 97*, 5185−5190.
9. Loo, J. A. (2000) Electrospray Ionization Mass Spectrometry: a Technology for Studying Noncovalent Macromolecular Complexes, *Int. J. Mass Spectrom. 200*, 175−186.
10. Ganem, B., and Henion, J. D. (2003) Going gently into flight: analyzing noncovalent interactions by mass spectrometry, *Bioorg. Med. Chem. 11*, 311−314.
11. Nemirovskiy, O. V., Ramanathan, R., and Gross, M. L. (1997) Investigation of Calcium-Induced, Noncovalent Association of Calmodulin with Melittin by Electrospray Ionization Mass Spectrometry, *J. Am. Soc. Mass Spectrom. 8*, 809−812.
12. Vis, H., Heinemann, U., Dobson, C. M., and Robinson, C. V. (1998) Detection of a Monomeric Intermediate Associated with Dimerization of Protein Hu by Mass Spectrometry, *J. Am. Chem. Soc. 120*, 6427−6428.
13. Kaltashov, I. A., and Eyles, S. J. (2002) Studies of Biomolecular Conformations and Conformational Dynamics by Mass Spectrometry, *Mass Spectrom. Rev. 21*, 37−71.
14. Light-Wahl, K. J., Schwartz, B. L., and Smith, R. D. (1994) Observation of the Noncovalent Quaternary Association of Proteins by Electrospray Ionization Mass Spectrometry, *J. Am. Chem. Soc. 116*, 5271−5278.
15. Apostol, I. (1999) Assessing the relative stabilities of engineered hemoglobins using electrospray mass spectrometry, *Anal. Biochem. 272*, 8−18.
16. Ofori-Acquah, S. F., Green, B. N., Davies, S. C., Nicolaides, K. H., Sarjeant, G. R., and Layton, D. M. (2001) Mass spectral analysis of asymmetric hemoglobin hybrids: demonstration of Hb FS ($\alpha_2\gamma\beta^s$) in sickle cell disease, *Anal. Biochem. 298*, 76−82.
17. Schmidt, A., and Karas, M. (2001) The Influence of Electrostatic Interactions on the Detection of Heme-Globin Complexes in ESI-MS, *J. Am. Soc. Mass Spectrom. 12*, 1092−1098.
18. Griffith, W. P., and Kaltashov, I. A. (2003) Highly asymmetric interactions between globin chains during hemoglobin assembly revealed by electrospray ionization mass spectrometry, *Biochemistry 42*, 10024−10033.
19. Fändrich, M., Tito, M. A., Leroux, M. R., Rostom, A. A., Hartl, F. U., Dobson, C. M., and Robinson, C. V. (2000) Observation of the noncovalent assembly and disassembly pathways of the chaperone complex MtGimC by mass spectrometry, *Proc. Natl. Acad. Sci. U.S.A. 97*, 14151−14155.
20. Simmons, D. A., and Konermann, L. (2002) Characterization of Transient Protein Folding Intermediates During Myoglobin Reconstitution by Time-Resolved Electrospray Mass Spectrometry with On-Line Isotopic Pulse Labeling, *Biochemistry 41*, 1906−1914.
21. Simmons, D. A., Dunn, S. D., and Konermann, L. (2003) Conformational Dynamics of Partially Denatured Myoglobin Studied by Time-Resolved Electrospray Mass Spectrometry With Online Hydrogen−Deuterium Exchange, *Biochemistry 42*, 5896−5905.
22. Versluis, C., and Heck, A. J. R. (2001) Gas-phase dissociation of hemoglobin, *Int. J. Mass Spectrom. 210/211*, 637−649.
23. Wilson, D. J., and Konermann, L. (2003) A Capillary Mixer With Adjustable Reaction Chamber Volume for Millisecond Time-Resolved Studies by Electrospray Mass Spectrometry, *Anal. Chem. 75*, 6408−6414.
24. Tahallah, N., Pinkse, M., Maier, C. S., and Heck, A. J. R. (2001) The effect of the source pressure on the abundance of ions of noncovalent protein assemblies in an electrospray ionization orthogonal time-of-flight instrument, *Rapid Commun. Mass Spectrom. 15*, 596−601.
25. Chernushevich, I. V., and Thomson, B. A. (2004) Collisional cooling of large ions in electrospray mass spectrometry, *Anal. Chem. 76*, 1754−1760.
26. Sobott, F., Hernandez, H., McCammon, M. G., Tito, M. A., and Robinson, C. V. (2002) A Tandem Mass Spectrometer for Improved Transmission and Analysis of Large Macromolecular Assemblies, *Anal. Chem. 74*, 1402−1407.
27. Pain, R. H. (2000) *Mechanisms of Protein Folding*, 2nd ed., Oxford University Press, New York.
28. Berberan-Santos, M. N., and Martinho, J. M. G. (1990) The Integration of Kinetic Rate Equations by Matrix Methods, *J. Chem. Educ. 67*, 375−379.
29. Beechem, J. M., Ameloot, M., and Brand, L. (1985) Global and Target Analysis of Complex Decay Phenomena, *Anal. Instrum. 14*, 379−402.
30. Holzwarth, A. R. (1995) Time-Resolved Fluorescence Spectroscopy, *Methods Enzymol. 246*, 334−362.
31. Konermann, L., Rosell, F. I., Mauk, A. G., and Douglas, D. J. (1997) Acid-Induced Denaturation of Myoglobin Studied by Time-Resolved Electrospray Ionization Mass Spectrometry, *Biochemistry 36*, 6448−6454.
32. Konermann, L., Collings, B. A., and Douglas, D. J. (1997) Cytochrome *c* Folding Kinetics Studied by Time-Resolved Electrospray Ionization Mass Spectrometry, *Biochemistry 36*, 5554−5559.
33. Konermann, L., Gatzen, G., and Holzwarth, A. R. (1997) Primary Processes and Structure of the Photosystem II Reaction Center. 5. Modeling of the Fluorescence Kinetics of the D1-D2-cytb559 Complex at 77 K, *J. Phys. Chem. B 101*, 2933−2944.
34. Green, B. N., and Vinogradov, S. N. (2004) An Electrospray Ionization Mass Spectrometric Study of the Subunit Structure of the Giant Hemoglobin from the Leech *Nephelopsis oscura*, *J. Am. Soc. Mass Spectrom. 15*, 22−27.
35. Babu, K. R., and Douglas, D. J. (2000) Methanol-Induced Conformations of Myoglobin at pH 4.0, *Biochemistry 39*, 14702−14710.
36. van Berkel, W. J. H., van den Heuvel, R. H. H., Versluis, C., and Heck, A. J. R. (2000) Detection of intact megadalton protein assemblies of vanillyl-alcohol oxidase by mass spectrometry, *Protein Sci. 9*, 435−439.
37. Feng, R., and Konishi, Y. (1993) Stepwise Refolding of Acid-Denatured Myoglobin: Evidence from Electrospray Mass Spectrometry, *J. Am. Soc. Mass Spectrom. 4*, 638−645.
38. Creighton, T. E. (1993) *Proteins*, W. H. Freeman & Co, New York.
39. Vogt, W. (1995) Oxidation of methionyl residues in proteins: tools, targets, and reversal, *Free Radical Biol. Med. 18*, 93−105.
40. Mueser, T. C., Rogers, P. H., and Arnone, A. (2000) Interface Sliding As Illustrated by the Multiple Quaternary Structures of Liganded Hemoglobin, *Biochemistry 39*, 15353−15364.
41. Sogbein, O. O., Simmons, D. A., and Konermann, L. (2000) The Effects of pH on the Kinetic Reaction Mechanism of Myoglobin Unfolding Studied by Time-Resolved Electrospray Ionization Mass Spectrometry, *J. Am. Soc. Mass Spectrom. 11*, 312−319.

42. Dobo, A., and Kaltashov, I. A. (2001) Detection of Multiple Protein Conformational Ensembles in Solution via Deconvolution of Charge-State Distributions in ESI MS, *Anal. Chem. 73*, 4763−4773.
43. Grandori, R. (2002) Detecting equilibrium cytochrome *c* folding intermediates by electrospray ionization mass spectrometry: Two partially folded forms populate the molten globule state, *Protein Sci. 11*, 453−458.
44. Nienhaus, G. U., Müller, J. D., McMahon, B. H., and Frauenfelder, H. (1997) Exploring the conformational landscape of proteins, *Physica D 107*, 297−311.
45. Rai, D. K., Landin, B., Alvelius, G., and Griffiths, W. J. (2002) Electrospray tandem mass spectrometry of intact β-chain hemoglobin variants, *Anal. Chem. 74*, 2097−2102.
46. Li, Y.-T., Hsieh, Y.-L., Henion, J. D., and Ganem, B. (1993) Studies on Heme Binding in Myoglobin, Hemoglobin, and Cytochrome *c* by Ion Spray Mass Spectrometry, *J. Am. Soc. Mass Spectrom. 4*, 631−637.
47. Mohimen, A., Dobo, A., Hoerner, J. K., and Kaltashov, I. A. (2003) A Chemometric Approach to Detection and Characterization of Multiple Protein Conformers in Solution Using Electrospray Ionization Mass Spectrometry, *Anal. Chem. 75*, 4139−4147.
48. Cech, N. B., and Enke, C. G. (2001) Practical Implication of Some Recent Studies in Electrospray Ionization Fundamentals, *Mass Spec. Rev. 20*, 362−387.
49. Yamaguchi, T., Pang, J., Reddy, K. S., Witkowska, H. E., Surrey, S., and Adachi, K. (1996) Expression of soluble human β-globin chains in bacteria and assembly *in vitro* with α-globin chains, *J. Biol. Chem. 271*, 26677−26683.
50. Vasudevan, G., and McDonald, M. J. (1997) Spectral demonstration of semihemoglobin formation during CN-hemin incorporation into human apohemoglobin, *J. Biol. Chem. 272*, 517−524.
51. Sridevi, K., and Udgaonkar, J. B. (2003) Surface Expansion Is Independent of and Occurs Faster than Core Solvation during the Unfolding of Barstar, *Biochemistry 42*, 1551−1563.

BI048501A